

## Cation ordering in epitaxial lead zirconate titanate films

L. C. Zhang,<sup>1</sup> A. L. Vasiliev,<sup>2</sup> I. B. Misirlioglu,<sup>3</sup> R. Ramesh,<sup>4</sup> S. P. Alpay,<sup>1</sup> and M. Aindow<sup>1,a)</sup>

<sup>1</sup>Department of Chemical, Materials and Biomolecular Engineering and Institute of Materials Science, University of Connecticut, Storrs, Connecticut 06269, USA

<sup>2</sup>Institute of Crystallography, Russian Academy of Sciences, Leninskij pr., 59, 119333 Moscow, Russia

<sup>3</sup>Materials Science and Engineering, Faculty of Engineering and Natural Sciences, Sabanci University, Tuzla, 34956 Istanbul, Turkey

<sup>4</sup>Department of Materials Science and Engineering and Department of Physics, University of California, Berkeley, California 94720, USA

(Received 23 October 2008; accepted 6 December 2008; published online 29 December 2008)

Electron diffraction and atom location by channeling enhanced microanalysis were used to show that epitaxial  $\text{PbZr}_{0.2}\text{Ti}_{0.8}\text{O}_3$  films grown on (001)  $\text{SrTiO}_3$  substrates by pulsed laser deposition exhibit long-range order on the tetravalent cation sublattice parallel to the film/substrate interface. This ordering gives two distinct tetravalent cation sites, one Zr lean and one Zr rich, and results in a superlattice with a tetragonal unit cell with lattice parameters  $a_0 \approx \sqrt{2}a_{\text{PZT}}$  and  $c_0 \approx a_{\text{PZT}}$ . Since such ordered states are inherently unstable in homovalent perovskite solutions, it is inferred that the ordering arises in response to the lattice misfit and could constitute an additional relaxation mode.  
© 2008 American Institute of Physics. [DOI: 10.1063/1.3058755]

Ferroelectric materials have received considerable interest in recent years due to their numerous potential device applications as elements of nonvolatile random access memories, dynamic random access memories, high dielectric constant capacitors, optical waveguides, tunable devices, and pyroelectric detectors. The electrical and electromechanical properties of ferroelectric films may differ significantly from those of the bulk single-crystal form due to the presence of internal stresses.<sup>1</sup> Internal stresses arise for several reasons in ferroelectric films including: the lattice mismatch between film and the substrate for epitaxial films, differences between the thermal expansion coefficients of the film and substrate, the self-strain of the ferroelectric phase transformation if the material is grown above the phase transformation temperature, and microstresses due to defects. In order to relieve the internal stresses that develop during film growth and subsequent cooling, complex defect structures are formed including: polydomains, antiphase boundaries, interfacial misfit dislocations, and threading dislocations (see, e.g., Ref. 2 and the references therein). These complicated microstructures evolve to relieve the internal stresses that develop during film growth and subsequent cooling from the deposition temperature. In this study, we report transmission electron microscopy (TEM) evidence for long-range cation ordering parallel to the interface plane in epitaxial (001)  $\text{PbZr}_{0.2}\text{Ti}_{0.8}\text{O}_3$  (PZT) films deposited on (001) single-crystal  $\text{SrTiO}_3$  (STO) substrates by pulsed laser deposition (PLD). Our results suggest that the ordering occurs in response to the stresses in the film and could, therefore, be considered as an additional relaxation mechanism.

Epitaxial PZT films of ~300 nm in thickness were grown by PLD onto Sr–O terminated Crystech (001) STO substrates using a 248 nm KrF pulsed excimer laser. The growth conditions used were those that have been shown previously to result in high quality epitaxial films with the orientation relationship:  $(001)_{\text{PZT}} \parallel (001)_{\text{STO}}$  and  $[100]_{\text{PZT}} \parallel [100]_{\text{STO}}$ .<sup>2</sup> Briefly, the substrates were cleaned with methanol and ac-

etone in an ultrasonic cleaner followed by a surface reflectivity check using an optical microscope. The substrates were heated to 600 °C and films were deposited from a PZT ceramic target using a pulse repetition rate of 5 Hz and a pulse energy of 600 mJ under an  $\text{O}_2$  partial pressure of 100 mTorr. The chamber was then backfilled with  $\text{O}_2$  before allowing the films to cool to room temperature at a rate of 5 °C/min. For TEM studies, plan-view and cross-sectional specimens were prepared by mechanical prethinning followed by  $\text{Ar}^+$  ion-beam milling to perforation with liquid nitrogen ( $\text{LN}_2$ ) cooling. Plan-view specimens were thinned from the substrate side only with a thin glass cover slip placed over the deposit side during milling to prevent redeposition onto the sample surface. Microstructural observations and microanalysis experiments were performed in a JEOL JEM-2010 FasTEM operating at 200 kV and equipped with an EDAX Phoenix ultrathin-window energy-dispersive x-ray spectrometer (EDXS).

Examples of the TEM data from these films are shown in Fig. 1. The bright-field TEM images obtained from the plan-view and cross-sectional specimens [e.g., Figs. 1(a) and 1(d), respectively] confirmed that the films are single crystal and that they contain a wide range of microstructural features including embedded *a*-oriented domains lying on the {101} planes and very high densities ( $\geq 10^{10} \text{ cm}^{-2}$ ) of threading dislocations. The character and origins of these features have been discussed in detail elsewhere.<sup>2–5</sup> Selected area diffraction patterns (SADPs) obtained with the beam direction **B** parallel to [001] in regions of the plan-view specimen with no *a*-oriented domains [e.g., Fig. 1(b)] exhibited strong 100- and 110-type diffraction maxima as expected for PZT. In these samples, however, the SADPs contained additional weak  $\frac{1}{2}\frac{1}{2}0$ -type maxima. Since these maxima were also present in SADPs obtained from samples tilted away from [001] along the 110-type systematic rows [e.g., Fig. 1(c)], they cannot be due to some high-order plural scattering effect and must correspond to the development of an ordered superlattice structure. Interestingly, these maxima were only observed in  $(\frac{1}{2}h, \frac{1}{2}k, 0)$  positions (where  $h, k = 2n + 1$ ), but

<sup>a)</sup>Electronic mail: m.aindow@uconn.edu.

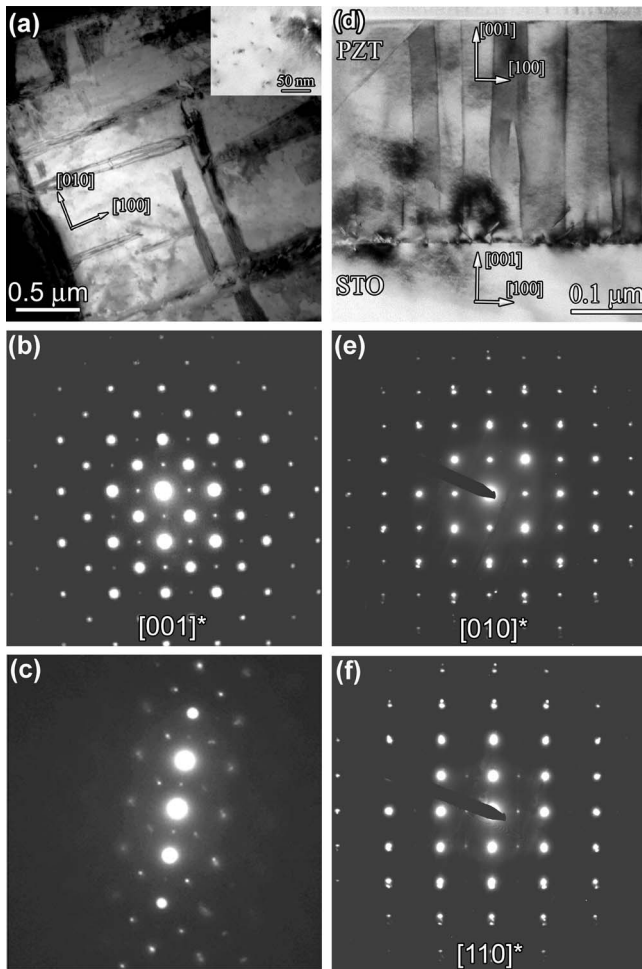


FIG. 1. TEM data obtained from plan-view [(a)–(c)] and cross-sectional [(d)–(f)] TEM specimens: (a) bright-field image obtained with  $\mathbf{B} \approx [001]$ , (b)  $[001]$  zone-axis SADP, (c) SADP obtained from the same region as (b) by tilting away from  $[001]$  along the  $1\bar{1}0$  Kikuchi band, (d) bright-field image obtained with  $\mathbf{B} \approx [010]$ , (e)  $[010]$  zone-axis SADP, and (f)  $[110]$  zone-axis SADP.

never in  $(\frac{1}{2}h, 0, \frac{1}{2}l)$  or  $(0, \frac{1}{2}k, \frac{1}{2}l)$  positions. Figures 1(e) and 1(f) are SADPs obtained from cross-sectional specimens with  $\mathbf{B} = [100]$  and  $[1\bar{1}0]$ , respectively; only the maxima expected for PZT are observed in Fig. 1(e), whereas Fig. 1(f) contains weak  $\frac{1}{2}\frac{1}{2}0$ -type maxima as observed in patterns from the plan-view samples. Thus, the superlattice structure corresponds to ordering parallel to  $(001)$ , i.e., parallel to the interface between the film and the substrate. We note that this ordering was sensitive to the specimen preparation conditions: no superlattice maxima were observed in SADPs from samples ion-milled at higher accelerating voltages or with no  $LN_2$  cooling. Moreover, there was some evidence for local electron-beam-induced disordering as the intensity of the superlattice reflections from a particular sample area decreased with increasing observation time.

In general, superlattice structures can be formed by displacive and/or replacive ordering. For PZT there are several possible ways in which structural ordering could occur including cation polarization with antiparallel  $[110]_P$  displacements of the Pb cations,<sup>6</sup> ordering of Zr and Ti on the tetravalent cation sublattice,<sup>7</sup> ordering of oxygen vacancies on the anion sublattice,<sup>8</sup> or coordinated rotations of oxygen octahedra.<sup>9,10</sup> From the ease with which the superlattice

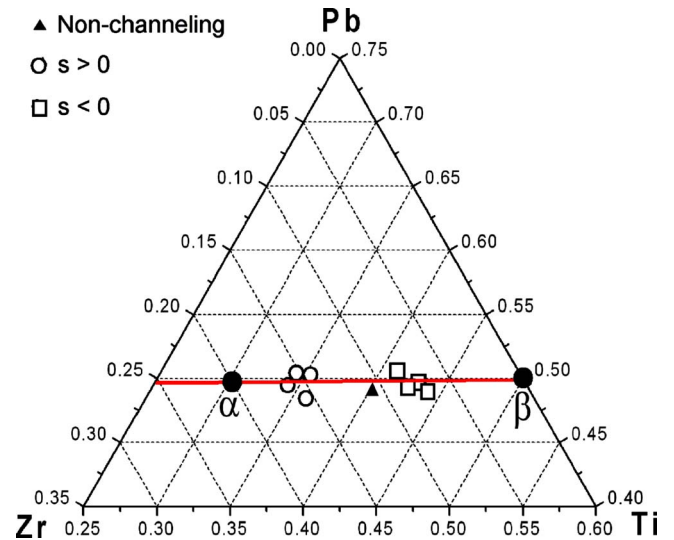


FIG. 2. (Color online) Partial Pb–Zr–Ti ternary section showing the ALCHEMI data obtained from the ordered PZT film including the compositions measured using EDXS at nonchanneling and channeling orientations, the best-fit OTL, and the limiting compositions for the most highly ordered state possible.

maxima were detected and their persistence in tilting experiments, it was deduced that cation ordering was the most likely explanation for this effect and EDXS-based atom location by channeling enhanced microanalysis (ALCHEMI) experiments were performed to test this hypothesis.

The EDXS data were obtained from regions that contained no  $a$ -oriented domains. The samples were first tilted toward the detector to minimize x-ray absorption effects and for each region an EDXS spectrum was acquired at a non-channeling orientation to verify the overall cation chemistry of the film. Planar ALCHEMI data were then acquired by reorienting the sample to give two-beam conditions for the operative diffraction vector  $\mathbf{g}$  and then acquiring spectra at positive and negative deviations  $s$  from the Bragg condition. A strong channeling effect ( $\approx 10\%$ ) was observed in such experiments with the cation compositions measured with  $s > 0$  for  $\mathbf{g} = \frac{1}{2}\frac{1}{2}0$  having more Ti but less Zr than the average and vice versa for  $s < 0$ . Figure 2 is a partial Pb–Ti–Zr ternary section showing the average composition measured from nonchanneling orientations and the individual compositions measured from channeling orientations. Following Hou *et al.*<sup>11</sup> a best-fit ordering tie line (OTL) was constructed passing through the average composition to indicate the sense of the ordering. Since the OTL lies at constant Pb content (50 at. %), the data confirm the ordering of Ti and Zr on the tetravalent cation sublattice. This ordering would give two distinct sites, one Zr rich and the other Zr lean; in the limit (i.e., in the most ordered state possible), these sites would have compositions 60% Ti, 40% Zr, and 100% Ti, respectively. These site composition limits are indicated in Fig. 2 by  $\alpha$  and  $\beta$ , respectively.

The only arrangement of these two tetravalent sites that is consistent with the diffraction data is the one shown in Fig. 3. Figure 3(a) is a projection along  $[001]$  showing an alternating arrangement of  $\alpha$  and  $\beta$  sites in  $(001)$  such that each of the  $(110)$  planes contains all  $\alpha$  or all  $\beta$  sites and similarly for  $(1\bar{1}0)$ . The unit cell for the resulting superlattice structure

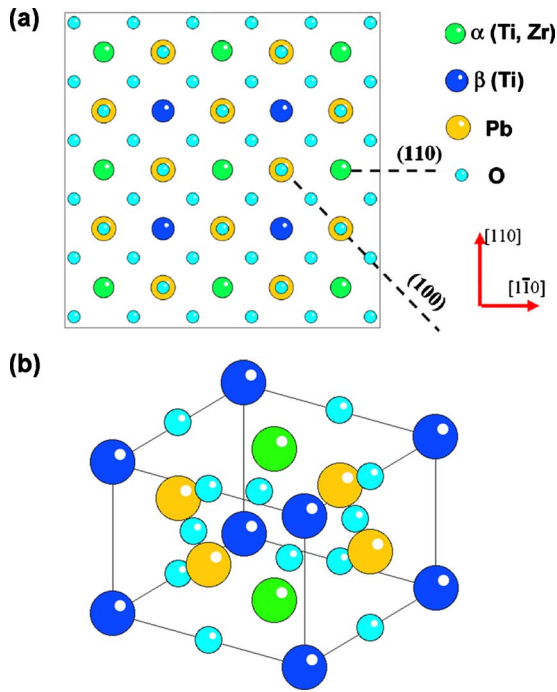


FIG. 3. (Color online) Structural model for the ordered superstructure: (a) [001] projection showing the partitioning of Zr onto half of the original tetraivalent sites and (b) tetragonal unit cell of the ordered superstructure.

is shown in Fig. 3(b): this is tetragonal with lattice parameters  $a_0 \approx \sqrt{2}a_{\text{PZT}}$  and  $c_0 \approx a_{\text{PZT}}$ .

The observation of a previously unreported ordered state is remarkable for a system such as PZT, which has been studied so extensively. Both  $\text{PbTiO}_3$  and  $\text{PbZrO}_3$  have the prototypical  $\text{ABO}_3$  perovskite lattice.  $\text{PbTiO}_3$  transforms from a cubic paraelectric to a tetragonal ferroelectric phase at  $490^\circ\text{C}$  upon cooling.  $\text{PbZrO}_3$ , on the other hand, displays an antiferroelectric phase transformation at around  $240^\circ\text{C}$ . PZT compounds ( $\text{PbZr}_{1-x}\text{Ti}_x\text{O}_3$ ) with  $x > 0.5$  are ferroelectric with a tetragonal crystal lattice at room temperature, whereas in compounds with  $x < 0.5$ , two variants of a rhombohedral phase may exist. For PZT with  $x \approx 0.5$ , it has also been proposed a monoclinic phase could form at the so-called morphotropic phase boundary (MPB),<sup>12</sup> although recent theoretical studies show that this phase might be a mixture of tetragonal and rhombohedral phases instead.<sup>13</sup> It is clear that the phases that form in the PZT system depend critically on the arrangement of the Zr and Ti atoms in the solid solution. Cation ordering, not only in PZT but also in several relaxor ferroelectrics,<sup>14</sup> has been a topic of great scientific and technological interest because these materials have an extremely high piezoelectric response, especially near MPBs. Theoretical results show that the formation of the different phases in the PZT system might be explained via atomic displacements (or “ordering”) due to electrostatic interactions between ions.<sup>15,16</sup> However, the positive enthalpy of mixing in the PZT system throughout the entire composition range,<sup>17</sup> the common observation of two phase mixtures near the MPB,<sup>18</sup> and comparative TEM studies of PZT with relaxor ferroelectrics<sup>19</sup> indicate that there is no tendency for chemical ordering of Zr and Ti ions at the B site of the PZT lattice. The apparent contradiction of this conclusion with the experimental observations of chemical order

presented here can be reconciled if one considers the possible influence of the substrate on the PZT thin film. There have been several reports of misfit-strain-induced long-range ordering in epitaxial semiconductor thin films (e.g., Refs. 20–22), whereby the change in the lattice parameter associated with the formation of the ordered state serves to relax partially the misfit between the thin film and substrate. It seems likely that similar effects are responsible for the superlattice structure in the present case since the ordering occurs only parallel to the interface plane, and the deposit disorders readily during TEM sample preparation and/or observation when the constraint of the substrate is removed.

Thus, the formation of the ordered state shown in Fig. 3 may constitute an additional mode of misfit stress relaxation in PZT. While it is difficult to estimate the degree of relaxation that this would provide, we note that this should be more significant where the conventional stress relaxation mechanisms, such as misfit dislocation and polydomain generation, are suppressed. This might apply for ultrathin epitaxial films and/or in films where the eigenstrain of the ferroelectric phase transformation is small.

The work at UConn was supported by the National U.S. Army Research Office through Grant No. W911NF-05-1-0528 and by the American Chemical Society, The Petroleum Research Fund.

- <sup>1</sup>D. G. Schlom, L.-Q. Chen, C.-B. Eom, K. M. Rabe, S. K. Streiffer, and J.-M. Triscone, *Annu. Rev. Mater. Res.* **37**, 589 (2007).
- <sup>2</sup>I. B. Misirlioglu, A. L. Vasiliev, M. Aindow, S. P. Alpay, and R. Ramesh, *J. Mater. Sci.* **41**, 697 (2006).
- <sup>3</sup>B. S. Kwak, A. Erbil, J. D. Budai, M. F. Chisholm, L. A. Boatner, and B. J. Wilkens, *Phys. Rev. B* **49**, 14865 (1994).
- <sup>4</sup>S. P. Alpay and A. L. Roytburd, *J. Appl. Phys.* **83**, 4714 (1998).
- <sup>5</sup>I. B. Misirlioglu, A. L. Vasiliev, M. Aindow, S. P. Alpay, and R. Ramesh, *Appl. Phys. Lett.* **84**, 1742 (2004); I. B. Misirlioglu, S. P. Alpay, M. Aindow, and V. Nagarajan, *ibid.* **88**, 102906 (2006).
- <sup>6</sup>J. Ricote, D. L. Corker, R. W. Whatmore, S. A. Impey, A. M. Glazer, J. Dec, and K. Roleder, *J. Phys.: Condens. Matter* **10**, 1767 (1998).
- <sup>7</sup>J. Frantti, S. Ivanov, J. Lappalainen, S. Eriksson, V. Lantto, S. Nishio, M. Kakihana, and H. Rundlof, *Ferroelectrics* **266**, 73 (2002).
- <sup>8</sup>J. F. Scott and M. Dawber, *Appl. Phys. Lett.* **76**, 3801 (2000).
- <sup>9</sup>Ragini, S. K. Mishra, D. Pandey, H. Lemmens, and G. Van Tendeloo, *Phys. Rev. B* **64**, 054104 (2001).
- <sup>10</sup>B. Noheda, L. Wu, and Y. Zhu, *Phys. Rev. B* **66**, 060103 (2002).
- <sup>11</sup>D. H. Hou, I. P. Jones, and H. L. Fraser, *Philos. Mag. A* **74**, 741 (1996).
- <sup>12</sup>B. Noheda, D. E. Cox, G. Shirane, J. A. Gonzalo, L. E. Cross, and S.-E. Park, *Appl. Phys. Lett.* **74**, 2059 (1999).
- <sup>13</sup>Y. M. Jin, Y. U. Wang, A. G. Khachatryan, J. F. Li, and D. Viehland, *Phys. Rev. Lett.* **91**, 197601 (2003); G. A. Rossetti, Jr., W. Zhang, and A. G. Khachatryan, *Appl. Phys. Lett.* **88**, 072912 (2006); G. A. Rossetti, Jr. and A. G. Khachatryan, *ibid.* **91**, 072909 (2007).
- <sup>14</sup>See, e.g., P. K. Davies, *Curr. Opin. Solid State Mater. Sci.* **4**, 467 (1999) and references therein.
- <sup>15</sup>L. Bellaiche and D. Vanderbilt, *Phys. Rev. Lett.* **81**, 1318 (1998).
- <sup>16</sup>I. Grinberg, V. R. Cooper, and A. M. Rappe, *Nature (London)* **419**, 909 (2002).
- <sup>17</sup>M. V. Rane, A. Navrotsky, and G. A. Rossetti, Jr., *J. Solid State Chem.* **161**, 402 (2001).
- <sup>18</sup>K. A. Schönau, L. A. Schmitt, M. Knapp, H. Fuess, R.-A. Eichel, H. Kungl, and M. J. Hoffmann, *Phys. Rev. B* **75**, 184117 (2007).
- <sup>19</sup>C. A. Randall, A. S. Bhalla, T. R. Shrout, and L. E. Cross, *J. Mater. Res.* **5**, 829 (1990).
- <sup>20</sup>T. S. Kuan, T. F. Kuech, W. I. Wang, and E. L. Wilkie, *Phys. Rev. Lett.* **54**, 201 (1985).
- <sup>21</sup>A. Ourmazd and J. C. Bean, *Phys. Rev. Lett.* **55**, 765 (1985).
- <sup>22</sup>P. B. Littlewood, *Phys. Rev. B* **34**, 1363 (1986).